Natural Antioxidants

DOI: 10.1002/anie.201407995

Short-lived Phenoxyl Radicals Formed from Green-Tea Polyphenols and Highly Reactive Oxygen Species: An Investigation by Time-Resolved EPR Spectroscopy**

*Dmytro Neshchadin, Stephen N. Batchelor, Itzhak Bilkis, and Georg Gescheidt**

Abstract: *Polyphenols are effective antioxidants and their behavior has been studied in depth. However, a structural characterization of the species formed immediately upon hydrogen-atom transfer (HAT), a key reaction of oxidative stress, has not been achieved. The reaction of catechin and green-tea polyphenols with highly reactive O-centered H-abstracting species was studied at the molecular level and in real time by using time-resolved electron paramagnetic resonance (EPR) spectroscopy. This mirrors the reaction of highly reactive oxygen species with polyphenols. The results show that all phenolic OH groups display essentially identical reactivity. Accordingly, there is no site specificity for HAT and initial antioxidative events are demonstrated to be largely ruled by statistical (entropic) factors.*

Oxidative stress and its prevention by antioxidants are active areas of research with applications in many different fields of research, ranging from the molecular sciences to medicine. In terms of our everyday life, it has been recognized for many years that tea is a good source of antioxidants.[1] Many experiments have sought to assess the antioxidant potential of tea ingredients, particularly polyphenols. A key conclusion is that polyphenols act as potent antioxidants to radical attack through hydrogen-atom abstraction (HAT) from the phenolic OH groups.[2,3]

Three selected major polyphenols [catechin (**CA**), gallocatechin (**GC**), and epigallocatechingallate (**EGCG**)] of green tea are presented in Figure 1. In most cases, ring A has two phenolic OH groups in a resorcinol-type *meta* arrangement. Typically, the B ring has either two *ortho* OH groups, representing a catechol moiety, or three neighboring OH substituents. In contrast to the A, B, and D rings, the OH group at the C ring is not phenolic.

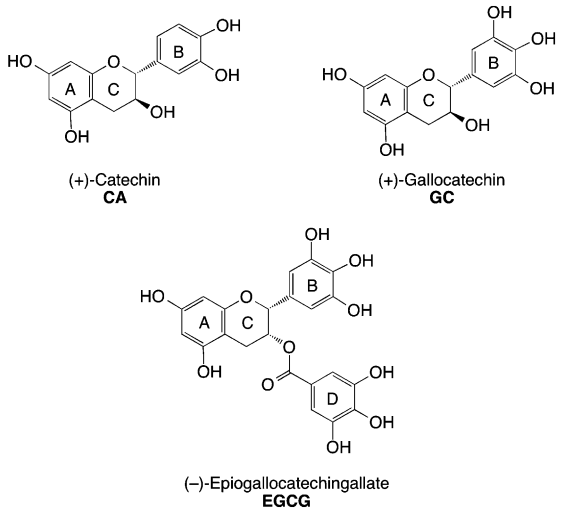

Figure 1. Selected major green-tea polyphenols.

Steady-state electron paramagnetic resonance (EPR) spectroscopy has been used to probe the molecular background of antioxidant properties,[4–7] and some metabolites originating from the oxidation of tea polyphenols have been identified.[8,9] On the basis of these investigations, the catechol or gallate moieties are thought to be central to the antioxidant properties of these compounds because they form thermodynamically favored phenoxyl radicals (and radical ions), which are produced through hydrogen abstraction by a reactive oxygen species (ROS) and stabilized by hydrogen bonding.[7,10–13]

On the other hand, investigations by pulse radiolysis performed on the ns timescale indicate that the A ring probably contributes to the antioxidative activity of tea polyphenols.[14–16] Since these conclusions were drawn from UV/Vis absorption spectra of short-lived intermediates, it was difficult to characterize their molecular structure unambiguously.[5] Accordingly, it is essential to choose methods that provide an unequivocal assignment of active intermediates at the molecular level and at an appropriate timescale.

Our initial results, obtained through time-resolved (500 ns–1 ms) and steady-state ^{1}H CIDNP spectroscopy, an NMR-derived method, suggested that hydrogen abstraction

[*] Dr. D. Neshchadin, Prof. Dr. G. Gescheidt
Institute of Physical and Theoretical Chemistry
Graz University of Technology, NAWI Graz
Stremayrgasse 9, 8010 Graz (Austria)
E-mail: g.gescheidt-demner@tugraz.at
Dr. S. N. Batchelor
Unilever Research Port Sunlight
Quarry Road East, Bebington, Wirral CH63 3JW (UK)
Prof. Dr. I. Bilkis
Institute of Biochemistry, Food Science & Nutrition
Faculty of Agriculture, Food & Environment
The Hebrew University of Jerusalem, POB 12
76100, Rehovot (Israel)

[**] G.G. and D.N. are indebted to NAWI Graz for support. We would like to thank the reviewers for several very helpful suggestions.

Supporting information for this article (experimental details, hyperfine data used for EPR simulations including those of B-ring radical **RB** (exp. and calc.), summary of additional radicals, which might be generated, TR-EPR spectra taken with **AQS** as the abstracting agent, and CIDNP spectra recorded from mixtures of catechol and resorcinol in the presence of benzophenone) is available on the WWW under http://dx.doi.org/10.1002/anie.201407995.

appears to proceed randomly.[17] However, the CIDNP technique only identifies the short-lived radical intermediates indirectly. We used time-resolved electron paramagnetic resonance (TR-EPR) to provide structural characterization of short-lived radicals at the ns time scale, appropriate for the diffusion-controlled reaction between antioxidants like polyphenols and, for example, alkoxyl or hydroxyl radicals, which are among the most reactive ROS present in nature.

Benzophenone (**BP**) and the disodium salt of 9,10-anthraquinone-2,6-disulfonic acid (**AQS**) are ideal reactants for testing antioxidative properties since, in their triplet states, they display a HAT reactivity matching that of highly reactive ROS.[18–22] The triplet state of **BP**/**AQS** is attained through excitation with light (laser flash at 355 nm, 6–8 ns), and it reacts with the polyphenol to form the corresponding primary radicals in their ground state (Scheme 1). These short-lived

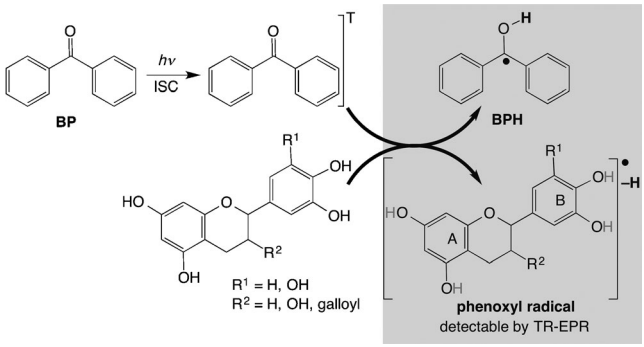

Scheme 1. Generation of phenoxyl-type radicals through the use of **BP**.

radicals are detected by TR-EPR to obtain a fingerprint[23] formed in the ns timescale. The exact structure of the radicals can be derived from the EPR parameters (through hyperfine coupling constants; hfcs) matched to DFT calculations.

Figure 2 shows the TR-EPR spectrum obtained upon laser-flash photolysis of **BP** and **CA** in a water/acetonitrile (5:1) mixture at pH 5.6. A range of distinct resonances is

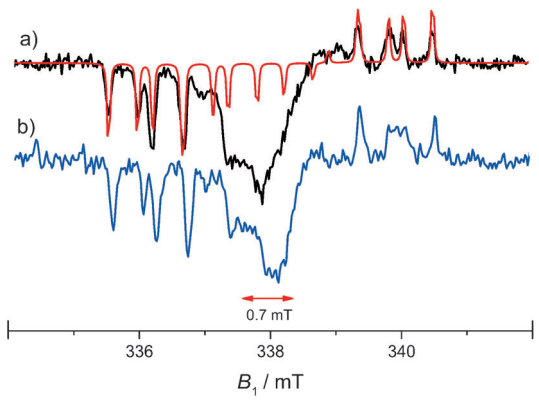

Figure 2. TR-EPR spectrum for a) **CA**/**BP** (black) and a simulation of the EPR spectrum attributed to **RB** (red). b) TR-EPR spectrum for **CA**/[D_{10}]-**BP** (room temperature, solvent H_2O/MeCN 5:1, pH 5.6). The red arrow indicates 0.7 mT (see text). The corresponding spectra with **AQS** are shown in the Supporting Information.

observed for both enhanced emission and absorption because of magnetic field effects, which substantially enhance the sensitivity of the method.[24] Herein, we will concentrate on the hyperfine pattern of the EPR signals.

The EPR spectra are dominated by a component with markedly large ^{1}H isotropic hfcs of 2.67, 1.15, 0.67, and 0.44 mT, each of which corresponds to one hydrogen atom (as indicated by the simulation; red line, Figure 2). EPR Spectra of radicals obtained upon oxidation (e.g., by O_2) of alkaline solutions containing polyphenols[4,7,25–27] have widths of approximately 0.7 mT, typical for catechol- or gallate-type radicals. However, the TR-EPR spectrum has an overall width of 4.93 mT. Accordingly, it cannot be attributed to a B-ring radical.

Owing to this spectral width being broader by a factor of approximately seven, the A-ring-based radicals are likely candidates for the dominating component of the TR-EPR signal. Two radicals, **RA1** and **RA2**, in which either one of the phenolic H atoms is abstracted, have to be considered. The calculated hfcs (calculated by DFT, which generally leads to a very reliable prediction of experimentally determined hfcs[28–31]) of these two radicals are given in Figure 3.

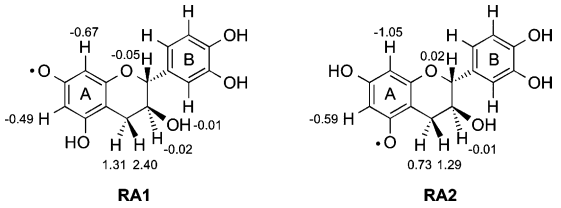

Figure 3. Radicals **RA1** and **RA2** and calculated hfcs (B3LYP/TZVP, in mT).

The computational prediction for radical **RA1** reveals the highest hfcs for the two methylene protons (β positions) adjacent to the A ring (1.31, 2.40 mT), followed by the aromatic protons of ring A (0.49, 0.67 mT), while the remaining ^{1}H hfcs are negligibly small (Figure 3). A similar spin distribution exists for **RA2,** but the β-hydrogen atoms possess markedly smaller hfcs (0.73, 1.29 mT). Consequently, the EPR for **RA1** will give rise to a substantially broader spectrum than that for **RA2** (4.9 vs. 3.7 mT). Indeed, the EPR data for the broad spectrum are in very good agreement with the calculated counterparts for **RA1** (*calc.* vs. exp.): *2.40*/2.67, *1.31*/1.15, *0.67*/0.67, and *0.49*/0.44 mT. Consequently, time-resolved EPR clearly identifies an A-ring-based phenoxyl radical.

The central, poorly-resolved feature of the EPR spectrum must consist of several components. Counter radical **BPH** (see Scheme 1), which is detectable at the short time scale of our experiment, certainly contributes to this part of the spectrum. The ketyl radical **BPH** has a narrow EPR spectrum (^{1}H hfcs of ca. 0.3 (1 H, OH), 0.12 (4 H, *m*), 0.36 (2 H, *p*), and 0.32 (4 H, *o*) mT; width ca. 2.8 mT).[32,33] This is further borne out by using deuterated [D_{10}]-**BP**, for which the shape of the central signal is altered because of the much smaller ^{2}H hfcs compared to ^{1}H (factor 0.12, width ca. 0.34 mT).

However, even with [D_{10}]-**BP**, a broad signal remains. This can be ascribed to lines from **RA1** (red spectrum, Figure 2) and to the well-established B-ring radical **RB** (and, possibly, to additional radicals with narrow EPR spectra, see above and the Supporting Information).[4,7,25–27] The composition of the experimental spectrum based on the above components is displayed in Figure 4.

Assuming correct assignment, the spectra should be pH dependent to reflect different degrees of phenolic deprotonation, and this was indeed observed (Figure 5). The EPR spectrum at pH 8.1 differs from that at pH 5.6, while that at pH 6.8 is an overlay of the two spectra.

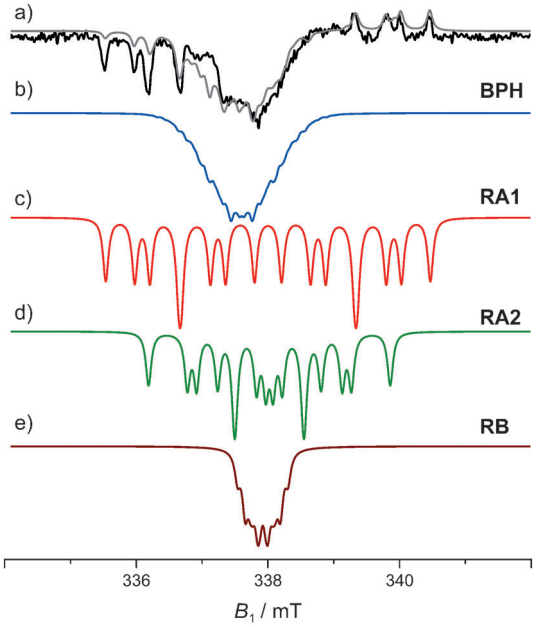

Figure 4. Components of the central part of the EPR signal displayed in Figure 2: a) experimental TR-EPR spectrum for **CA**/**BP** at pH 5.6 (black) and the corresponding simulation (grey), b) simulation for **BPH** (blue),[33] c) simulation for **RA1** (red), d) simulation for **RA2** (green), and e) simulation for **RB** (brown) The simulations are based on calculated hfcs, which are in good agreement with experimental ones, where these are available (see the Supporting Information).

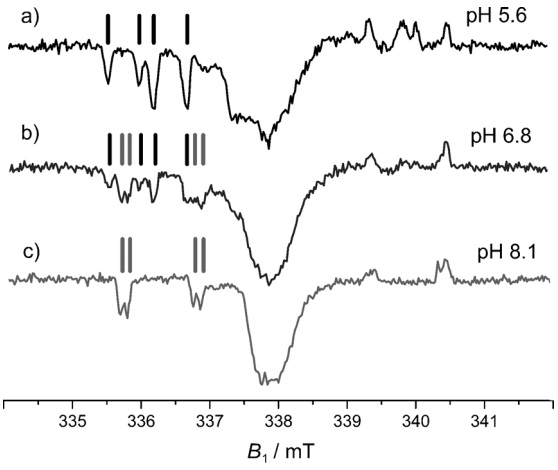

Figure 5. pH-dependent EPR spectra for **CA**/**BP** at different pH values: a) pH 5.6, b) pH 6.8, and c) pH 8.1.

At pH 5.6, the A ring is fully protonated, it becomes singly deprotonated at pH 8.1, and an equilibrium between these forms is present at pH 6.8.[34–37] Hydrogen-atom abstraction at pH 8.1 is expected to lead to radical $\mathbf{RA}^-$, with calculated values for $\mathbf{RA}^-$ being in good agreement with the experimental ones. Three positions show distinct hfcs, the highest of which are predicted for the A-ring β positions (*calc.*/exp.: *2.41*/2.53 and *1.36*/1.05 mT) and for one of the aromatic protons at the A ring (*1.10*/1.05 mT; Figure 6). This observation supports the generation of A-ring phenoxyl radicals by HAT.

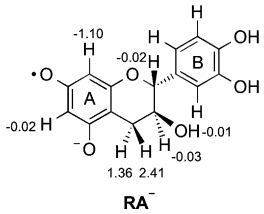

Figure 6. Radical anion $\mathbf{RA}^-$ (calculated hfcs, B3LYP/TZVP, in mT).

These results reveal different radicals to those detected by steady-state EPR upon the oxidation of alkaline polyphenol solutions. It is therefore crucial to test whether the photolysis of **CA**/**BP** solutions is compatible with the hitherto published measurements. We therefore performed the photoreaction between **BP** and **CA** with standard EPR detection at pH 8.1. The spectra thus obtained are substantially different from those obtained on the 50 ns timescale. However, the spectra taken on a timescale of minutes, which show a width of approximately 0.7 mT, perfectly correspond to those reported when alkaline solutions of **CA** are reacted with atmospheric oxygen and are ascribed to B-ring-based radicals (see the Supporting Information).[4,7,25–27,38,39] This result unequivocally demonstrates that the timescale of detection is crucial to the nature of the observed radicals.

The above-described experiments show the reactivity of **CA** as a model system. A key question is whether such a reactivity also holds for real-world beverages, such as green tea. To answer this, we brewed green tea under typical consumer conditions to provide an aqueous solution rich in polyphenols but also many more components, such as carbohydrates, simple acids, and proteins. To match the reaction conditions for **CA**, the pH values were adjusted to the physiological range. Figure 7 shows the TR-EPR spectra obtained for green tea under the same experimental conditions as those shown in Figure 5. Remarkably, the outermost lines are identical for the "real" and the reference system and the pH dependence also matches. The remarkable intensity of the outermost lines reflects the fact that most of the naturally occurring polyphenols possess a resorcinol-type A ring. This unequivocally shows that A-ring radicals are formed when green tea responds to highly reactive ROS that produce HAT.

Our results indicate that kinetic effects direct the initial reaction pathways when highly reactive oxygen-centered radicals attack polyphenols, in other words, these radicals

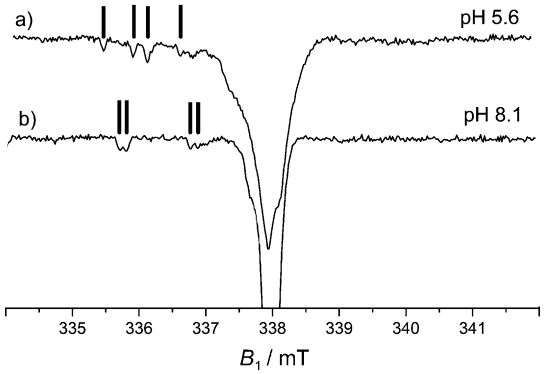

Figure 7. TR-EPR spectra taken upon laser-flash photolysis of an **AQS**/green tea mixture. a) pH 5.6; b) pH 8.1.

do not act as site-specific agents. Without any doubt, the bond-dissociation enthalpy of phenolic compounds depends upon electronic factors and hydrogen bonding.[29,40–44] However, when there is a competitive situation between several phenolic groups within one molecule, stochastic factors dominate the early stages of the (anti)oxidative action rather than thermodynamic factors.

In an additional experiment, we examined this entropic aspect. We photolyzed an 1:1 mixture of resorcinol and catechol in the presence of **BP** and followed this reaction by ^{1}H-CIDNP spectroscopy (see the Supporting Information). Although resorcinol-based phenoxyl radicals are thermodynamically less stable than catechol-derived ones, the CIDNP technique revealed short-lived radicals based on both components.

In summary, our experiments show that polyphenol-based antioxidants cannot simply be characterized according to thermodynamic factors, for example, the bond-dissociation energies of the phenolic O–H bonds. Thermodynamically less stable resorcinol-type A ring radicals are clearly present upon high oxidative stress. Kinetic effects explain the formation of several metabolites found in published investigations.[45–47] Moreover, such short-timescale phenomena representing a subtle interplay between kinetic and thermodynamic factors are decisive in several (anti)oxidative processes because polyphenols with nonconjugated (poly)phenolic moieties can react with highly reactive ROS at more than one active site independently.

Non-specific hydrogen abstraction at short timescales produces persistent *and* reactive phenoxyl radicals. Remarkably, this is consistent with classifications derived from the TEAC assay.[48] Resorcinol-type radicals[3,46,49,50] formed at short timescales may cause harmful effects.[4,51]

Received: August 6, 2014
Revised: September 6, 2014
Published online: October 24, 2014

Keywords: antioxidants · EPR spectroscopy · oxidative stress · polyphenols · radicals

[1] L. R. Juneja, M. P. Kapoor, T. Okubo, T. P. Rao, *Green Tea Polyphenols: Nutraceuticals of Modern Life*, CRC, Boca Raton, FL, **2013**.
[2] S. Quideau, D. Deffieux, C. Douat-Casassus, L. Pouysegu, *Angew. Chem. Int. Ed.* **2011**, *50*, 586 – 621; *Angew. Chem.* **2011**, *123*, 610 – 646.
[3] C. Rice-Evans, N. J. Miller, G. Paganga, *Free Radical Biol. Med.* **1996**, *20*, 933 – 956.
[4] A. E. Hagerman, R. T. Dean, M. J. Davies, *Arch. Biochem. Biophys.* **2003**, *414*, 115 – 120.
[5] W. Bors, C. Michel, *Free Radical Biol. Med.* **1999**, *27*, 1413 – 1426.
[6] V. Butković, L. Klasinc, W. Bors, *J. Agric. Food Chem.* **2004**, *52*, 2816 – 2820.
[7] J. F. Severino, B. Goodman, C. W. M. Kay, K. Stolze, D. Tunega, T. G. Reichenauer, K. F. Pirker, *Free Radical Biol. Med.* **2009**, *46*, 1076 – 1088.
[8] J. V. Higdon, B. Frei, *Crit. Rev. Food Sci. Nutr.* **2003**, *43*, 89 – 143.
[9] J. van Duynhoven, E. E. Vaughan, D. M. Jacobs, R. A. Kemperman, E. J. J. van Velzen, G. Gross, L. C. Roger, S. Possemiers, A. K. Smilde, J. Dore, J. A. Westerhuis, T. Van de Wiele, *Proc. Natl. Acad. Sci. USA* **2011**, *108*, 4531 – 4538.
[10] M. Matxain Jon, D. Padro, M. Ristila, A. Strid, A. Eriksson Leif, *J. Phys. Chem. B* **2009**, *113*, 9629 – 9632.
[11] E. Nazarparvar, M. Zahedi, E. Klein, *J. Org. Chem.* **2012**, *77*, 10093 – 10104.
[12] T. Yoshida, K. Hirozumi, M. Harada, S. Hitaoka, H. Chuman, *J. Org. Chem.* **2011**, *76*, 4564 – 4570.
[13] P. Mulder, H.-G. Korth, D. a. Pratt, G. a. DiLabio, L. Valgimigli, G. F. Pedulli, K. U. Ingold, *J. Phys. Chem. A* **2005**, *109*, 2647 – 2655.
[14] S. V. Jovanovic, Y. Hara, S. Steenken, M. G. Simic, *J. Am. Chem. Soc.* **1995**, *117*, 9881 – 9888.
[15] S. V. Jovanovic, S. Steenken, M. Tosic, B. Marjanovic, M. G. Simic, *J. Am. Chem. Soc.* **1994**, *116*, 4846 – 4851.
[16] C. Cren-Olivé, P. Hapiot, J. Pinson, C. Rolando, *J. Am. Chem. Soc.* **2002**, *124*, 14027 – 14038.
[17] D. Neshchadin, R. Levinn, G. Gescheidt, S. N. Batchelor, *Chem. Eur. J.* **2010**, *16*, 7008 – 7016.
[18] C. Evans, J. C. Scaiano, K. U. Ingold, *J. Am. Chem. Soc.* **1992**, *114*, 4589 – 4593.
[19] D. Griller, J. A. Howard, P. R. Marriott, J. C. Scaiano, *J. Am. Chem. Soc.* **1981**, *103*, 619 – 623.
[20] T. Yoshihara, M. Yamaji, T. Itoh, H. Shizuka, T. Shimokage, S. Tero-Kubota, *Phys. Chem. Chem. Phys.* **2000**, *2*, 993.
[21] N. K. Bridge, G. Porter, *Proc. R. Soc. London Ser. A* **1958**, *244*, 259 – 275.
[22] A. Bedini, E. De Laurentiis, B. Sur, V. Maurino, C. Minero, M. Brigante, G. Mailhotc, D. Vione, *Photochem. Photobiol. Sci.* **2012**, *11*, 1445 – 1453.
[23] M. Brustolon, E. Giamello, *Electron Paramagnetic Resonance: A Practitioner's Toolkit*, Wiley, Hoboken, **2009**.
[24] S. Nagakura, H. Hayashi, T. Azumi, *Dynamic Spin Chemistry*, Kodansha and Wiley, Tokyo and New York, **1998**.
[25] M. Adams, M. S. Blois, R. H. Sands, *J. Chem. Phys.* **1958**, *28*, 774 – 776.
[26] T. Oniki, U. Takahama, *J. Wood Sci.* **2004**, *50*, 545 – 547.
[27] J. A. Pedersen, *CRC Handbook of EPR Spectra from Quinones and Quinols*, CRC, Boca Raton, FL, **1985**.
[28] V. Barone, P. Cimino, E. Stendardo, *J. Chem. Theory Comput.* **2008**, *4*, 751 – 764.
[29] R. Amorati, G. F. Pedulli, M. Guerra, *Org. Biomol. Chem.* **2010**, *8*, 3136 – 3141.
[30] L. Hermosilla, P. Calle, J. M. G. de La Vega, C. Sieiro, *J. Phys. Chem. A* **2005**, *109*, 1114 – 1124.
[31] R. Batra, B. Giese, M. Spichty, G. Gescheidt, K. N. Houk, *J. Phys. Chem.* **1996**, *100*, 18371 – 18379.

[32] A. Kawai, T. Hidemori, K. Shibuya, *Chem. Phys. Lett.* **2005**, *414*, 378 – 383.
[33] R. Wilson, *J. Chem. Soc. B* **1968**, 84 – 90.
[34] S. V. Jovanovic, S. Steenken, Y. Hara, M. G. Simic, *J. Chem. Soc. Perkin Trans. 2* **1996**, 2497 – 2504.
[35] S. Steenken, P. Neta, *J. Phys. Chem.* **1979**, *83*, 1134 – 1137.
[36] M. Callaghan Rose, J. Stuehr, *J. Am. Chem. Soc.* **1968**, *90*, 7205 – 7209.
[37] M. Eigen, *Angew. Chem. Int. Ed. Engl.* **1964**, *3*, 1 – 19; *Angew. Chem.* **1963**, *75*, 489 – 508.
[38] J. A. Kuhnle, J. J. Windle, A. C. Waiss, *J. Chem. Soc. B* **1969**, 613 – 616.
[39] O. N. Jensen, J. A. Pedersen, *Tetrahedron* **1983**, *39*, 1609 – 1615.
[40] R. Amorati, G. F. Pedulli, *Org. Biomol. Chem.* **2012**, *10*, 814 – 818.
[41] G. Litwinienko, P. Mulder, *J. Phys. Chem. A* **2009**, *113*, 14014 – 14016.
[42] L. Valgimigli, R. Amorati, S. Petrucci, G. F. Pedulli, D. Hu, J. J. Hanthorn, D. A. Pratt, *Angew. Chem. Int. Ed.* **2009**, *48*, 8348 – 8351; *Angew. Chem.* **2009**, *121*, 8498 – 8501.
[43] V. Thavasi, R. P. A. Bettens, L. P. Leong, *J. Phys. Chem. A* **2009**, *113*, 3068 – 3077.
[44] K. U. Ingold, D. A. Pratt, *Chem. Rev.* **2014**, *114*, 9022 – 9046.
[45] L. Ridder, J. J. J. van der Hooft, S. Verhoeven, R. C. H. de Vos, R. J. Bino, J. Vervoort, *Anal. Chem.* **2013**, *85*, 6033 – 6040.
[46] J. J. J. van der Hooft, R. C. H. de Vos, V. Mihaleva, R. J. Bino, L. Ridder, N. de Roo, D. M. Jacobs, J. P. M. van Duynhoven, J. Vervoort, *Anal. Chem.* **2012**, *84*, 7263 – 7271.
[47] J. Perez-Jimenez, J. Hubert, L. Hooper, A. Cassidy, C. Manach, G. Williamson, A. Scalbert, *Am. J. Clin. Nutr.* **2010**, *92*, 801 – 809.
[48] K. Mukai, S. Mitani, K. Ohara, S.-I. Nagaoka, *Free Radical Biol. Med.* **2005**, *38*, 1243 – 1256.
[49] M. Arts, J. S. Dallinga, H. P. Voss, G. Haenen, A. Bast, *Food Chem.* **2004**, *88*, 567 – 570.
[50] P. K. Das, M. V. Encinas, J. C. Scaiano, *J. Am. Chem. Soc.* **1981**, *103*, 4154 – 4162.
[51] J. T. Fox, S. Sakamuru, R. Huang, N. Teneva, S. O. Simmons, M. Xia, R. R. Tice, C. P. Austin, K. Myung, *Proc. Natl. Acad. Sci. USA* **2012**, *109*, 5423 – 5428.

